Critical Points of the Electric Field from a Collection of Point Charges

Nelson Max[1] and Tino Weinkauf[2]

[1] Lawrence Livermore National Laboratory, 7000 East Avenue, Livermore, CA, 94550, USA, max2@llnl.gov
[2] Zuse Institute Berlin, Takustr. 7, D-14195 Berlin, Germany, weinkauf@zib.de

1 Introduction

The electric field around a molecule is generated by the charge distribution of its constituents: positively charged atomic nuclei, which are well approximated by point charges, and negatively charged electrons, whose probability density distribution can be computed from quantum mechanics [Ba90]. For the purposes of molecular mechanics or dynamics, the charge distribution is often approximated by a collection of point charges, with either a single partial charge at each atomic nucleus position, representing both the nucleus and the electrons near it, or as several different point charges per atom.

The critical points in the electric field are useful in visualizing its geometrical and topological structure, and can help in understanding the forces and motion it induces on a charged ion or neutral dipole. Most visualization tools for vector fields use only samples of the field on the vertices of a regular grid, and some sort of interpolation, for example, trilinear, on the grid cells. There is less risk of missing or misinterpreting topological features if they can be derived directly from the analytic formula for the field, rather than from its samples. This work presents a method which is guaranteed to find all the critical points of the electric field from a finite set of point charges. To visualize the field topology, we have modified the saddle connector method of [Th03] to use the analytic formula for the field.

The analysis below would also apply to gravity in astronomy, since the Newtonian gravitational force outside a spherically symmetric body is the same as if all its mass were concentrated at its center.

2 Electric Potential and Field

The electrostatic potential $P(X)$ at position X, resulting from a point charge q at position A is

$$P(X) = \frac{q}{4\pi\epsilon|X-A|} = \frac{q}{4\pi\epsilon((X-A)\cdot(X-A))^{1/2}}$$

where ϵ is the permittivity of the medium. Since we are only interested in the field topology here, we will for simplicity below neglect the factor $4\pi\epsilon$. By definition, the electrostatic field F is the negative gradient of the potential, so, neglecting the factor $4\pi\epsilon$,

$$\begin{aligned} F(X) &= -\nabla \frac{q}{((X-A)\cdot(X-A))^{1/2}} \\ &= \frac{q(X-A)}{((X-A)\cdot(X-A))^{3/2}} \ . \end{aligned} \tag{1}$$

Therefore, for a set of n charges q_i at positions A_i, the electrostatic field is

$$F(X) = \sum_{i=1}^{n} \frac{q_i(X-A_i)}{((X-A_i)\cdot(X-A_i))^{3/2}} \ . \tag{2}$$

3 Octree Method for Finding Critical Points

Our method of finding critical points of F starts with a single cubical cell, or a regular grid of such cells, guaranteed as in section 4 to contain all the critical points of F. We describe below a test to prove that a cubical cell C contains no critical points of F. This test is based on computing component-wise bounds F^{max} and F^{min} for the possible values of $F(X)$ within the cell. In the column vectors F^{max} and F^{min}, if any of the three components are both positive or both negative, we know that $F(X)$ cannot be zero for any X in C, so there are no critical points of the field in C, the test passes, and the cell can be skipped. Otherwise, all of the components of $F(X)$ could possibly become zero inside C, and the test fails, so we divide the cell into eight equal subcells, and recursively test these subcells. Thus we converge on the critical points. At the limiting depth of the recursion, the centers of cells which fail the test are written to an output list. This list is then pruned by averaging clusters of points within a threshold distance of each other. (Currently, this threshold is taken as 6 times the edge length of the cell at the recursion limit.) The test will fail for cells containing any of the point charge locations, so these locations will also be on the output list. The octree is never explicitly stored, and the only memory it uses is for the portion in the stack for the recursion. By trading space for time, one could store the force at vertices in some local portion of the octree, saving some recomputation for neighboring cells.

Consider a cubical cell C of side s, with vertices V_{ijk}, where i, j, and k are either 0 or 1, and count along the x, y, and z axes respectively. Our goal

is to get bounds F^{max} and F^{min} on the values of $F(X)$ inside this cell, using the values of F on the eight vertices V_{ijk}, and bounds on the derivatives of F inside C. Since F is the negative gradient of the potential P, its derivatives are the entries in H, the negative of the Hessian matrix of second derivatives of the potential, *i.e.*

$$\mathsf{H}(X) = \sum_{i=1}^{n} \left(\frac{q_i \mathsf{I}}{|X - A_i|^{3/2}} - 3 \frac{q_i (X - A_i)(X - A_i)^\top}{|X - A_i|^{5/2}} \right) . \tag{3}$$

Here I is the identity matrix, and $(X - A_i)(X - A_i)^\top$ is a square matrix, since X and A_i are column vectors. Let H^j be the j^{th} row of H and F^j be the j^{th} component of the vector F. Let V be one of the vertices V_{ijk}, and let X be any point inside the cell. Applying the mean value theorem to the function $E^j(t) = F^j(V + t(X - V))$, for j = 1, 2, or 3, there is a value t_j with $0 \le t_j \le 1$, so that

$$F^j(X) = F^j(V) + \mathsf{H}^j(Y_j)(X - V) \tag{4}$$

where $Y_j = V + t_j(X - V)$. Therefore bounds on the entries of H will help us get bounds on the components of F.

Consider the denominators in equation (3). The quantity $|Y - A_i|$ attains its maximum in C at one of the vertices of the cube C. If A_i is not inside cell C, then $|Y - A_i|$ attains a positive minimum in C at a vertex of C, or at the projection of A_i on one of the faces or edges of C. (Cells containing a point charge A_i fail the test, and are recursively subdivided.)

For each point charge A_i and each of the 9 elements of H, we can find the upper and lower bounds for each of the two terms in equation (3), using either the minimum or the maximum value of the denominator, taking into account the multiple possible signs of the numerator, and its upper and lower bounds. By summing the bounds on these two terms over all the point charges, we can get element-wise upper and lower bounds H^{max} and H^{min} for the matrix $\mathsf{H}(Y)$.

Then, using each vertex V_{ijk} in equation (4), we can obtain component-wise upper and lower bounds F^{max}_{ijk} and F^{min}_{ijk} for $F(X)$ with X in C, by taking into account the signs of the components of the column vector factor $(X - V)$ in equation (4). For example, if V in equation (4) is V_{011}, then for X in C, $X - V$ is of the form $(x, y, z)^\top$, with $0 \le x \le s$, $-s \le y \le 0$, and $-s \le z \le 0$, so, as shown in 1D in figure 1, we get the component-wise bounds

$$\begin{aligned} F^{max}_{011} = {} & F(V_{011}) + \max(0, \mathsf{H}^{max}(s, 0, 0)^\top) + \max(0, \mathsf{H}^{min}(0, -s, 0)^\top) \\ & + \max(0, \mathsf{H}^{min}(0, 0, -s)^\top) , \end{aligned}$$

and

$$\begin{aligned} F^{min}_{011} = {} & F(V_{011}) + \min(0, \mathsf{H}^{min}(s, 0, 0)^\top) + \min(0, \mathsf{H}^{max}(0, -s, 0)^\top \\ & + \min(0, \mathsf{H}^{max}(0, 0, -s)^\top) . \end{aligned}$$

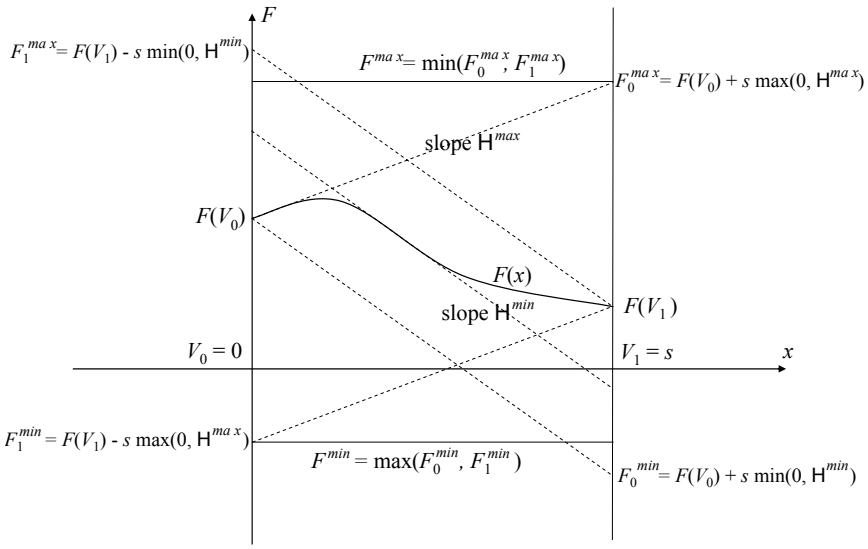

Fig. 1. A 1D example for computing bounds on a function $F(x)$.

Finally, let $F^{max} = \min_{ijk} F_{ijk}^{max}$ and $F^{min} = \max_{ijk} F_{ijk}^{min}$ be the componentwise minimum and maximum from these eight respective estimates, giving the tightest bounds they collectively impose on $F(X)$ in C. As described above, these bounds are used to limit the octree search. Note that in the 1D case illustrated in figure 1, $F^{max} > 0$, and $F^{min} < 0$, so further subdivision would be required. However, the lowest vertex of the parallelogram bounded by the dotted lines of slope H^{max} and H^{min} from $F(V_0)$ and $F(V_1)$ is above the $F = 0$ axis, so we could actually skip this cell. In 3D, the range of F values satisfying the eight pairs of linear inequalities could be found by low dimensional linear programming [deB00], but this is more complicated, and so far we have not done so.

4 Finding a Sphere Containing all the Critical Points

In order to make sure that all the critical points are found, we need to make the initial root cube or grid large enough to contain them all. We instead find a large enough sphere, and enclose it in the initial grid. To do this, we expand equation (2) into a series of terms, which decrease with different inverse powers of the distance $r = |X|$ of the point X from the origin. This series is closely related to the multipole expansion of the potential described in [Wiki], [Ja62],

or [Sch94], but is slightly different because we are expanding the field, and not the potential. We will find a sphere outside of which the first non-vanishing term of this series dominates the sum of the later terms, so that $F(X)$ cannot vanish.

Consider first a single point charge q at position A, as in equation (1), let $r = |X|$, and rewrite the denominator as follows:

$$\begin{aligned} F(X) &= \frac{q(X-A)}{((X-A)\cdot(X-A))^{3/2}} \\ &= \frac{q(X-A)}{(|X|^2 - 2A\cdot X + |A|^2)^{3/2}} \\ &= \frac{q(X-A)}{(r^2(1+\frac{1}{r^2}(-2A\cdot X + |A|^2))^{3/2}} \\ &= \frac{qr(\frac{X}{r} - \frac{A}{r})}{r^3\left(1+\left(\frac{|A|^2}{r^2} - 2\frac{A}{r}\cdot\frac{X}{r}\right)\right)^{3/2}} \\ &= \frac{q}{r^2}\left(\hat{X} - \frac{A}{r}\right)\left(1+\left(\frac{|A|^2}{r^2} - 2\frac{A}{r}\cdot\hat{X}\right)\right)^{-3/2}, \end{aligned} \tag{5}$$

where $\hat{X} = X/r$ is the unit vector in the direction of X. Let

$$t = \frac{|A|^2}{r^2} - 2\frac{A}{r}\cdot\hat{X}\ .$$

Then, expanding $(1+t)^{-3/2}$ by the binomial series (the same as its Taylor expansion about t = 0), which converges for $|t| < 1$, we get

$$\begin{aligned} (1+t)^{-3/2} &= \left(1 + (-3/2)t + (-3/2)(-5/2)t^2/2! + \cdots\right) \\ &= \sum_{l=0}^{\infty}\binom{-\frac{3}{2}}{l} t^l \end{aligned} \tag{6}$$

where the generalized binomial coefficient

$$\binom{s}{l} = \frac{s(s-1)(s-2)\cdots(s-l+1)}{l!}\ .$$

Substituting this binomial series into equation (5), and writing $A\cdot\hat{X}$ as $A^\top\hat{X}$, we have

$$\begin{aligned} F(X) = \frac{q}{r^2}\left(\hat{X} - \frac{A}{r}\right)\Bigg(1 + \left(-\frac{3}{2}\right)t + \left(-\frac{3}{2}\right)\left(-\frac{5}{2}\right)\frac{t^2}{2!} \\ + \cdots + \left(-\frac{3}{2}\right)\left(-\frac{5}{2}\right)\cdots\left(-\frac{2l+1}{2}\right)\frac{t^l}{l!} + \cdots\Bigg) \end{aligned} \tag{7}$$

$$
\begin{aligned}
&= \frac{q}{r^2}\left(\hat{X} - \frac{A}{r}\right)\left(1 + \left(-\frac{3}{2}\right)\left(\frac{|A|^2}{r^2} - 2\frac{A^\top \hat{X}}{r}\right)\right. \\
&\quad \left. + \left(-\frac{3}{2}\right)\left(-\frac{5}{2}\right)\left(\frac{|A|^2}{r^2} - 2\frac{A^\top \hat{X}}{r}\right)^2/2 + \cdots\right) \\
&= \frac{q}{r^2}\left(\hat{X} - \frac{A}{r}\right)\left(1 - \frac{3}{2}\left(\frac{|A|^2}{r^2} - 2\frac{A^\top \hat{X}}{r}\right)\right. \\
&\quad \left. + \frac{15}{8}\left(\frac{|A|^4}{r^4} - 4\frac{|A|^2}{r^3}A^\top \hat{X} + 4\frac{(A^\top \hat{X})^2}{r^2}\right) + \cdots\right) \\
&= \frac{q}{r^2}\left(\hat{X} - \frac{A}{r}\right)\left(1 - \frac{3}{2}\frac{|A|^2}{r^2} + 3\frac{A^\top \hat{X}}{r}\right. \\
&\quad \left. + \frac{15}{8}\frac{|A|^4}{r^4} - \frac{15}{2}\frac{|A|^2 A^\top \hat{X}}{r^3} + \frac{15}{2}\frac{\hat{X}^\top A A^\top \hat{X}}{r^2} + \cdots\right) \qquad (8)
\end{aligned}
$$

Using the distributive law to multiply out the two parenthesized factors in equation (8), and grouping terms with the same negative power of r, we get

$$
\begin{aligned}
F(X) = \frac{q\hat{X}}{r^2} + \frac{q(3(A^\top \hat{X})\hat{X} - A)}{r^3} \\
+ \frac{q}{r^4}\left(-\frac{3}{2}|A|^2\hat{X} - 3AA^\top \hat{X} + \frac{15}{2}(\hat{X}^\top AA^\top \hat{X})\hat{X}\right) + \cdots \quad . \qquad (9)
\end{aligned}
$$

In the case of several point charges, we sum over the point charges to get

$$
F(X) = \frac{q_{total}\hat{X}}{r^2} + \frac{3(D \cdot \hat{X})\hat{X} - D}{r^3} + \frac{\mathsf{M}\hat{X} + (\hat{X}^\top \mathsf{N}\hat{X})\hat{X}}{r^4} + \cdots \ , \qquad (10)
$$

where the total charge $q_{total} = \sum_{i=1}^{n} q_i$, the dipole moment $D = \sum_{i=1}^{n} q_i A_i$, and the 3 by 3 matrices

$$
\mathsf{M} = -3\sum_{i=1}^{n} q_i A_i A_i^\top - \left(\frac{3}{2}\sum_{i=1}^{n} q_i |A_i|^2\right)\mathsf{I}
$$

and

$$
\mathsf{N} = \frac{15}{2}\sum_{i=1}^{n} q_i A_i A_i^\top \ .
$$

The first monopole term in equation (10) is linear in $\hat{X}$, the second dipole term is quadratic in $\hat{X}$, the third quadrupole term is cubic in $\hat{X}$, and so on. The monopole and dipole terms are as in equation 1.2.8 of [Sch94].

4.1 The monopole case

There are several cases, depending on which of these terms is the first non-zero one. Our goal is to find the radius r_m of a sphere containing all the critical

points. If q_{total} is non-zero, we need to show that the magnitude $|q_{total}|/r^2$ of the monopole term is greater than the magnitude of the sum of all the rest of the terms, if $r > r_m$, for some appropriate r_m. If $q_{total} = 0$, we will instead use one of the higher order terms, as in sections 4.2 or 4.3.

We can bound the term in the line numbered (7) of the binomial series by

$$\left|\left(-\frac{3}{2}\right)\left(-\frac{5}{2}\right)\cdots\left(-\frac{2l+1}{2}\right)\frac{t^l}{l!}\right| \;=\; \frac{3}{2\times 1}\frac{5}{2\times 2}\cdots\frac{2l+1}{2\times l}|t|^l \;\le\; \left|\frac{3}{2}t\right|^l \;.$$

Then this binomial series is dominated by a geometric series, and the sum of all its terms after the first is dominated by the sum of the geometric series:

$$\sum_{l=1}^{\infty}\left|\binom{-\frac{3}{2}}{l}t^l\right| \;\le\; \sum_{l=1}^{\infty}\left|\frac{3}{2}t\right|^l = \frac{\left|\frac{3}{2}t\right|}{1-\left|\frac{3}{2}t\right|}\;.$$

For the i^{th} point charge, let

$$t_i = \frac{|A_i|^2}{r^2} - 2\frac{A_i}{r}\cdot\hat{X}\;.$$

If we chose $r_m \ge 8k|A_i|$, for an as yet undetermined $k \ge 1$, and if $r > r_m$, then

$$\begin{aligned}|t_i| &\le \frac{|A_i|^2}{(8k|A_i|)^2} + 2\frac{|A_i|}{8k|A_i|}\\ &\le \frac{1}{64k^2} + \frac{2}{8k} \;\le\; \frac{1}{64k} + \frac{2}{8k} \;=\; \frac{17}{64k}\end{aligned}$$

so, using the fact that $k \ge 1$

$$\begin{aligned}\left|\sum_{l=1}^{\infty}\binom{-\frac{3}{2}}{l}t_i^l\right| &\le \frac{\left|\frac{3}{2}t_i\right|}{1-\left|\frac{3}{2}t_i\right|}\\ &\le \frac{\frac{51}{128k}}{1-\frac{51}{128k}} \;\le\; \frac{\frac{51}{128k}}{1-\frac{51}{128}}\\ &\le \frac{\frac{51}{128k}}{\frac{77}{128}} \;=\; \frac{51}{77k}\;.\end{aligned}$$

If we take $r_m = \max_i(8k|A_i|)$, for $k = \sum_{i=1}^n |q_i|/|\sum_{i=1}^n q_i| \ge 1$, sum over the contributions of all the the point charges, use the inequality $|B-C| \ge |B|-|C|$ for any two vectors B and C, and use the fact that $|\hat{X}| = 1$, we get, for $r > r_m$,

$$\begin{aligned}|F(X)| &= \left|\sum_{i=1}^{n}\left(\frac{q_i}{r^2}\left(\hat{X}-\frac{A_i}{r}\right)(1+t_i)^{-3/2}\right)\right|\\ &= \left|\sum_{i=1}^{n}\left(\frac{q_i}{r^2}\left(\hat{X}-\frac{A_i}{r}\right)\left(1+\sum_{l=1}^{\infty}\binom{-\frac{3}{2}}{l}t_i^l\right)\right)\right|\end{aligned}$$

$$
\begin{aligned}
&= \left| \sum_{i=1}^{n} \frac{q_i}{r^2} \hat{X} - \left(\sum_{i=1}^{n} \frac{q_i}{r^2} \frac{A_i}{r} - \sum_{i=1}^{n} \frac{q_i}{r^2} \left(\hat{X} - \frac{A_i}{r} \right) \sum_{l=1}^{\infty} \binom{-\frac{3}{2}}{l} t_i^l \right) \right| \\
&\geq \left| \sum_{i=1}^{n} \frac{q_i}{r^2} \hat{X} \right| - \left| \sum_{i=1}^{n} \frac{q_i}{r^2} \frac{A_i}{r} - \sum_{i=1}^{n} \frac{q_i}{r^2} \left(\hat{X} - \frac{A_i}{r} \right) \sum_{l=1}^{\infty} \binom{-\frac{3}{2}}{l} t_i^l \right| \\
&\geq \left| \sum_{i=1}^{n} \frac{q_i}{r^2} \right| - \left(\sum_{i=1}^{n} \frac{|q_i|}{r^2} \frac{|A_i|}{8k|A_i|} + \sum_{i=1}^{n} \frac{|q_i|}{r^2} \left(1 + \frac{|A_i|}{8k|A_i|} \right) \frac{51}{77k} \right) \\
&= \frac{|\sum_{i=1}^{n} q_i|}{r^2} - \frac{\sum_{i=1}^{n} |q_i|}{r^2} \left(\frac{1}{8} + \frac{51}{77} \left(1 + \frac{1}{8k} \right) \right) \frac{|\sum_{i=1}^{n} q_i|}{\sum_{i=1}^{n} |q_i|} \\
&= \frac{|\sum_{i=1}^{n} q_i|}{r^2} \left(1 - \left(\frac{1}{8} + \frac{51}{77} \left(1 + \frac{1}{8k} \right) \right) \right) \\
&\geq \frac{|\sum_{i=1}^{n} q_i|}{r^2} \left(1 - \left(\frac{1}{8} + \frac{51}{77} \left(1 + \frac{1}{8} \right) \right) \right) \\
&= \frac{|\sum_{i=1}^{n} q_i|}{r^2} \left(1 - \frac{536}{616} \right) \\
&= \frac{|\sum_{i=1}^{n} q_i|}{r^2} \frac{80}{616} \\
&> 0 \,,
\end{aligned}
$$

and thus there are no critical points outside the sphere of radius r_m.

4.2 The dipole case

If the total charge q_{total} is zero, as on a neutral molecule, but the dipole moment D is non-zero, we can proceed similarly, getting a lower bound on the dipole term, and showing that it dominates the remaining terms outside of a sufficiently large sphere.

To get the lower bound on the dipole term $(3(D \cdot \hat{X})\hat{X} - D)/r^3$, note that the points in the set $\{(D \cdot \hat{X})\hat{X}\}$ lie on a sphere of diameter $|D|$ centered at the point $\frac{1}{2}D$, since the point $(D \cdot \hat{X})\hat{X}$ is the foot of the perpendicular line from the point D to the line from the origin in the direction $\hat{X}$. (See figure 2 for a 2D analog.) Thus the points of the form $3(D \cdot \hat{X})\hat{X}$ lie on a sphere of radius $\frac{3}{2}D$ centered at $\frac{3}{2}D$, and the translated points of the form $3(D \cdot \hat{X})\hat{X} - D$ lie on the translated sphere of radius $\frac{3}{2}D$ centered at $\frac{1}{2}D$. The closest point on this translated sphere to the origin is $-D$, and its distance to the origin is $|D|$. Thus a lower bound on the dipole term is $|D|/r^3$.

Since the dipole term arises from the terms $l = 0$ and $l = 1$ in the series (6) and (7), to show that the dipole dominates, we separate these terms from the remaining terms:

$$
F(X) = \sum_{i=0}^{n} \left(\frac{q_i}{r^2} \left(\hat{X} - \frac{A_i}{r} \right) \left(1 - \frac{3}{2} \left(\frac{|A_i|^2}{r^2} - 2 \frac{A_i^\top \hat{X}}{r} \right) + \sum_{l=2}^{\infty} \binom{-\frac{3}{2}}{l} t_i^l \right) \right.
$$

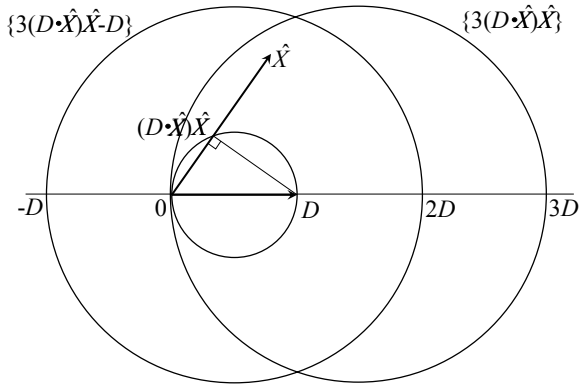

Fig. 2. Construction of the circle $\{3(D \cdot \hat{X})\hat{X} - D\}$ for all unit vectors $\hat{X}$.

$$= \frac{\sum_{i=0}^{n} q_i \hat{X}}{r^2} - \frac{\sum_{i=0}^{n} q_i A_i}{r^3} + \frac{3\left(\sum_{i=0}^{n} q_i A_i \cdot \hat{X}\right)\hat{X}}{r^3} - \frac{\frac{3}{2}\sum_{i=0}^{n} q_i |A_i|^2 \hat{X}}{r^4} - \frac{3\sum_{i=0}^{n} q_i A_i A_i^\top \hat{X}}{r^4} + \frac{\frac{3}{2}\sum_{i=0}^{n} q_i |A_i|^2 A_i}{r^5} + \sum_{i=0}^{n} \frac{q_i}{r^2}\left(\hat{X} - \frac{A_i}{r}\right)\sum_{l=2}^{\infty}\binom{-\frac{3}{2}}{l} t_i^l \,. \tag{11}$$

Of the seven terms in equation (11), the first is the monopole term, which we are assuming is zero, and the second and third are the dipole contribution, for which we just derived a lower bound. Similar to the monopole case, we can show that these dipole terms dominate the next three terms, because of their higher powers of r in the denominator, and also the last term, using the geometric series as above, if $r > r_m$, with

$$r_m = 36(\max_{i=1}^{n} |A_i|) \sum_{i=1}^{n} |q_i| / |D| \,. \tag{12}$$

4.3 The quadrupole case

If both the total charge q_{total} and the dipole moment D are zero, and the quadrupole term is not zero, then the electric field decreases as $1/r^4$. Unlike the dipole case, we have not been able to derive a simple lower bound on the magnitude of the quadrupole term in equation (10). Instead, we apply the techniques in section 3, using the mean value theorem to get a lower bound.

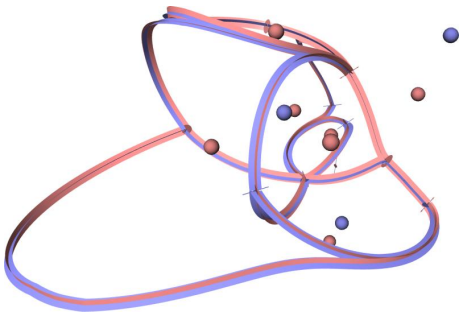

Fig. 3. The saddle connectors between the saddle points of an isolated alanine residue from a protein. The 10 atom centers are shown as pink spheres for sources (positive point charges), and blue spheres for sinks.

We cover the unit sphere with a regular 2D latitude longitude (θ, ϕ) grid. Then, for each 2D grid cell, we find its 3D axis-aligned bounding box. For this box, we find bounds on the entries of the 3 by 3 matrix Q for the partial derivatives of the vector-valued function

$$G(\hat{X}) = \mathsf{M}\hat{X} + (\hat{X}^\top \mathsf{N}\hat{X})\hat{X} \ ,$$

with respect to the 3D Cartesian coordinates of $\hat{X}$. By the chain rule, the 3 by 2 partial derivative matrix P of $G(\hat{X}(\theta, \phi))$ with respect to θ and ϕ is the product of Q and the 3 by 2 Jacobian matrix J for the function $\hat{X}(\theta, \phi)$. We use the minimum and maximum on the 2D grid cell for the entries of J together with the lower and upper bounds on the 3D bounding box for the entries of Q, to find bounds on the entries of P. A 2D version of the method in section 3 can then give the bounds on the components of the vector $G(\hat{X})$, and thus a lower bound for $|G(\hat{X})|$ over the 2D cell. Let B be the minimum of this lower bound over all the 2D grid cells covering the sphere. (For the examples in this paper, we directly found $B > 0$ for the initial grid, so quadtree subdivision was not needed.) Then the norm of the quadrupole term is

$$\left| \frac{\mathsf{M}\hat{X} + (\hat{X}^\top \mathsf{N}\hat{X})\hat{X}}{r^4} \right| \geq \frac{B}{r^4} \ .$$

The vanishing monopole and dipole terms and the non-vanishing quadrupole term come from the $l = 0$, 1, and 2 terms of the series in (6) and (7), so, as for the dipole case, one can show that the quadrupole term dominates the sum of the six other terms from taking $l = 0$, 1, and 2 in equation (7), plus the sum

$$\sum_{i=1}^{n} \frac{q_i}{r^2} \left(\hat{X} - \frac{A_i}{r} \right) \sum_{l=3}^{\infty} \binom{-\frac{3}{2}}{l} t_i^l \ ,$$

when $r > r_m$, with

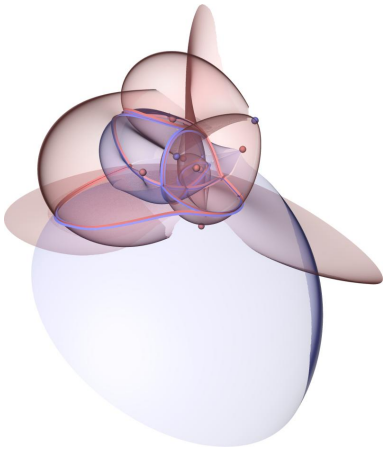

Fig. 4. The separation surfaces for the saddle points of an isolated alanine residue from a protein.

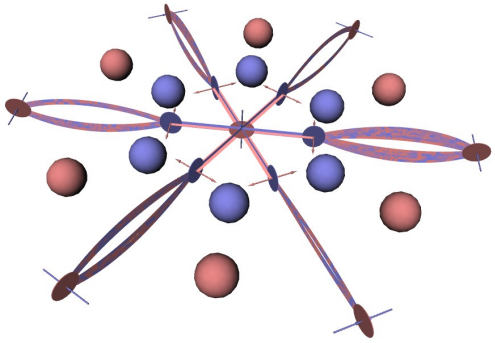

Fig. 5. The saddle connectors for a benzene molecule with 12 point charges.

$$r_m = \max\left(6\,\max_i|A_i|, \frac{61}{B}\sum_{i=1}^{n}|q_i||A_i|^3\right) . \tag{13}$$

We have not dealt with higher order cases, but they can be handled similarly, and are not normally needed.

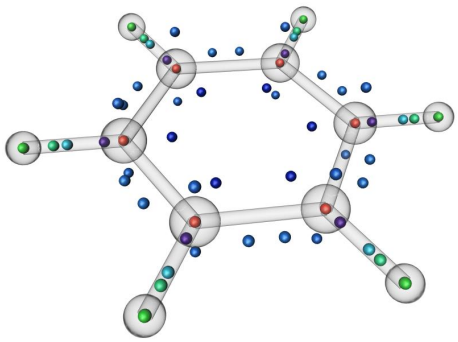

Fig. 6. A benzene molecule with 60 point charges.

5 Results

Figure 3 shows the saddle connectors between the critical points of an alanine residue isolated from a protein by cutting its peptide bonds. Standard partial charges making q_{total} zero were placed on the 10 atom centers, which are sources and sinks of the electric field. It took the 15 seconds on one processor of a dual 3.3 GHz Xeon workstation, to recursively search 457,328 octree cells to depth 44, and locate to 12 decimal place accuracy the 10 saddle points, using a sphere of size $r_m = 4$, known to contain all the critical points. However equation (12) gives $r_m = 238.4$, and then it took 14 hours to find the same critical points. Figure 4 shows the separation surface for this structure. These figures were drawn by a modification of the integration methods in [Th03] which uses the analytic gradient to integrate the separation surfaces and find the saddle connectors. Figure 5 shows the saddle connectors for a benzene molecule, with equal negative partial charges at each of its six carbon atoms, and positive charges at each of the six hydrogen atoms. Because of its symmetry, benzene has zero dipole moment as well as zero total charge, but it has a non-zero quadrupole moment.

The partial charge assignment at the atom positions gives only a rough approximation to the actual charge distribution generating the potential, and is certainly an oversimplification in the case of benzene, where the π orbitals from the carbon atoms lie above and below the plane of the 12 atom centers. We have obtained a more accurate quantum mechanical approximation of the electrostatic potential described in [St96], using 60 point charges. Figure 6 shows the arrangement of these point charges, which are not all in the same plane. It took 66 minutes to recursively search 23,290,456 octree cells to to a depth of 44 and find the 193 critical points, using $r_m = 4$. However equation (13) gives $r_m = 9633$, and with this value, the algorithm ran for a week without terminating. So the estimates (12) and (13) for r_m are not

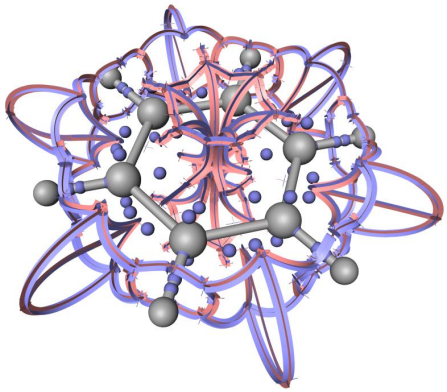

Fig. 7. The saddle connectors for a benzene molecule with 60 point charges.

very practical. Of the octree cells examined for $r_m = 4$, 14,833,200 were at level 8, while between 58,688 and 63,272 were at each of the levels 14 through 44. This shows that once the search locates the critical point neighborhood, the convergence is linear in the precision desired, and justifies our decision not to use a less robust method like Newton-Raphson iteration at the final stage. Figure 7 shows the saddle connectors for this collection of point charges, and figure 8 shows the separation surfaces. These figures are close to the corresponding figures in [Th03], which inspired the current work, but are different. In [Th03], the field was sampled on a 101^3 grid, and then trilinearly interpolated inside the grid cells. The critical points found for this interpolated field, using the methods of [Ma02], were 40 sinks, 12 sources, and 132 saddles. (Slightly different approximate numbers were reported in [Th03], but these are the counts gotten by rerunning that code on the same input.) We reran code in that paper on a 255^3 grid, and found 42 sinks, 12 sources, and 129 saddles, including 3 spurious saddles, one each in a face, an edge, and a vertex of the cube bounding the data volume. However, the analytic method described in the current paper found all 48 sinks and 12 sources at the input point charges, and 133 saddles. This includes 6 pairs of saddles and sinks, with the two so close together in each pair that they could not be resolved by the sampling method. Thus the analytic method is superior in this case.

6 Acknowledgments

This work was performed under the auspices of the U. S. Department of Energy by the University of California, Lawrence Livermore National Laboratory under contract number W-7405-ENG-48. We wish to thank Thomas Steinke for locating the data of the 60 point charges for benzene in an apparently lost old file, Daniel Laney, Hans-Christian Hege, and Frank Holzwarth for

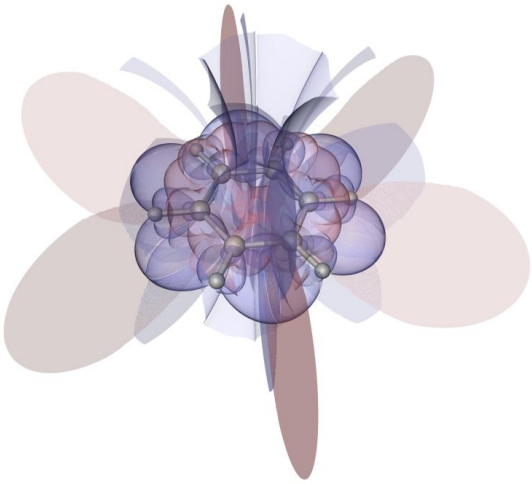

Fig. 8. The separation surfaces for a benzene molecule with 60 point charges.

help with LaTeX, and Ajith Mascarenhas and Hans-Christian Hege for reading the manuscript and making suggestions. All visualizations in this paper have been created using AMIRA – a system for advanced visual data analysis [Am05] (see `http://amira.zib.de/`).

References

[deB00] de Berg, M., van Kreveld, M., Overmars, M., Schwarzkopf, O.: Computational Geometry: Algorithms and Applications, Second Edition, Springer, Berlin, (2000)

[Am05] Stalling, D., Westerhoff, M., Hege, H.-C.: Amira: A Highly Interactive System for Visual Data Analysis. In: Hansen, C., Johnson, C. (eds) The Visualization Handbook, Elsevier, 749–767 (2005)

[Ba90] Bader, R.F.W.: Atoms in Molecules: A Quantum Theory. Clarendon Press, Oxford (1990)

[Ja62] Jackson, J. D.: Classical Electrodynamics. Wiley, New York (1962)

[Ma02] Mann, S., Rockwood, A.: Computing Singularities of 3D Vector Fields with Geometric Algebra. In: Moorhead, R., Gross, M., Joy, K (eds) Proceedings of IEEE Visualization 2002, 283–289 (2002)

[Sch94] Scharf, G.: From Electrostatics to Optics: A Concise Electrodynamics Course. Springer-Verlag, Berlin (1994)

[St96] Stalling, D., Steinke, T.: Visualization of Vector Fields in Quantum Chemistry. ZIB Preprint SC-96-01. ftp://ftp.zib.de/pub/zib-publications/reports/SC-96-01.ps

[Th03] Theisel, H., Weinkauf, T., Hege, H.-C., Seidel, H.-P.: Saddle Connectors - An Approach to Visualizing the Topological Skeleton of Complex 3D

Vector Fields. In: Turk, G, van Wijk, J.J., Moorhead, R. (eds) Proceedings of IEEE Visualization 2003, 225–232 (2003)

[Wiki] Wikipedia entry on spherical multipole moments. http://en.wikipedia.org/wiki/Spherical_multipole_moments